Journal of Structural Biology 192 (2015) 331–335

Contents lists available at ScienceDirect

Journal of Structural Biology

journal homepage: www.elsevier.com/locate/yjsbi

X-ray recordings reveal how a human disease-linked skeletal muscle α-actin mutation leads to contractile dysfunction

Julien Ochala [a,*], Gianina Ravenscroft [b], Elyshia McNamara [b], Kristen J. Nowak [b], Hiroyuki Iwamoto [c]

[a] Centre of Human and Aerospace Physiological Sciences, School of Biomedical Sciences, King's College London, London, United Kingdom
[b] Harry Perkins Institute of Medical Research, The University of Western Australia, Nedlands, Australia
[c] Japan Synchrotron Radiation Research Institute, SPring8, Hyogo, Japan

ARTICLE INFO

Article history:
Received 16 May 2015
Received in revised form 13 August 2015
Accepted 22 September 2015
Available online 25 September 2015

Keywords:
Muscle disease
Actin
Myosin
Small-angle X-ray scattering

ABSTRACT

In humans, mutant skeletal muscle α-actin proteins are associated with contractile dysfunction, skeletal muscle weakness and a wide range of primarily skeletal muscle diseases. Despite this knowledge, the exact molecular mechanisms triggering the contractile dysfunction remain unknown. Here, we aimed to unravel these. Hence, we used a transgenic mouse model expressing a well-described D286G mutant skeletal muscle α-actin protein and recapitulating the human condition of contractile deregulation and severe skeletal muscle weakness. We then recorded and analyzed the small-angle X-ray diffraction patterns of isolated membrane-permeabilized myofibers. Results showed that upon addition of Ca^{2+}, the intensity changes of the second (1/19 nm^{-1}) and sixth (1/5.9 nm^{-1}) actin layer lines and of the first myosin meridional reflection (1/14.3 nm^{-1}) were disrupted when the thin-thick filament overlap was optimal (sarcomere length of 2.5–2.6 μm). However these reflections were normal when the thin and thick filaments were not interacting (sarcomere length > 3.6 μm). These findings demonstrate, for the first time, that the replacement of just one amino acid in the skeletal muscle α-actin protein partly prevents actin conformational changes during activation, disrupting the strong binding of myosin molecules. This leads to a limited myosin-related tropomyosin movement over the thin filaments, further affecting the amount of cross-bridges, explaining the contractile dysfunction.

1. Introduction

In humans, more than 200 different mutations in the gene encoding skeletal muscle α-actin (*ACTA1*) have been identified and are associated with a wide range of skeletal muscle diseases including nemaline myopathy, cap disease, core myopathy, congenital fiber type disproportion and intranuclear rod myopathy (Nowak et al., 2013, 1999). Despite this diversity, almost all share one common feature, namely detrimental muscle weakness affecting limb and respiratory muscles (Nowak et al., 2013, 1999). No cure exists for patients and treatment focuses on symptomatic management such as respiratory intervention, particularly nocturnal ventilation (Nowak et al., 2013, 1999). Possible therapeutic approaches could be guided by the exact molecular mechanisms by which these *ACTA1* mutations lead to muscle diseases, however this information is currently lacking.

Most *ACTA1* mutations are relatively subtle, typically missense mutations modifying one DNA nucleotide. These in turn result in the substitution of just one residue in the skeletal muscle α-actin protein. Thus, understanding how such minor modifications induce muscle weakness, and more specifically contractile dysfunction, would give important insights into the pathophysiological phenomena. A few mouse models of *ACTA1* disease have been developed (Nguyen et al., 2011; Ravenscroft et al., 2011), including one that carries a D286G mutation (Ravenscroft et al., 2011). Skeletal muscle weakness in these mice has been linked to contractile deregulation characterized by an inappropriate amount of strongly bound myosin cross-bridges and decreased force-generating capacity (Ochala et al., 2012).

In skeletal muscle, myosin binding to thin filaments depends on other contractile proteins, e.g., tropomyosin. Indeed, in the absence of Ca^{2+}, tropomyosin sterically hinders interactions between actin and myosin molecules. Upon addition of Ca^{2+}, tropomyosin moves over the surface of actin exposing myosin-binding sites on thin

* Corresponding author at: Centre of Human & Aerospace Physiological Sciences, Faculty of Life Sciences and Medicine, King's College London, Room 3.3, Shepherd's House, Guy's Campus, London SE1 1UL, UK.
E-mail address: julien.ochala@kcl.ac.uk (J. Ochala).

http://dx.doi.org/10.1016/j.jsb.2015.09.008
1047-8477/

filaments, allowing the formation of strongly bound cross-bridges and the production of force (Lehman and Craig, 2008). One may hypothesize that D286G skeletal muscle α-actin alters some of the processes mentioned above. To investigate this, in the present study we recorded the X-ray diffraction patterns of single membrane-permeabilized myofibers from wild-type (WT) mice and from transgenic rodents expressing the D286G skeletal muscle α-actin mutation (referred to as D286G). We then monitored intensity changes during activation, and in various conditions. We measured the far off-meridional part of the second actin layer line (ALL) at 1/19 nm^{-1} (tropomyosin), sixth and seventh ALL at 1/5.9 and 1/5.1 nm^{-1}, respectively (actin). We also measured the first myosin meridional reflection (MM), at 1/14.3 nm^{-1} (myosin) .

2. Materials and methods

2.1. Animals

The Animal Experimentation Ethics Committee of The University of Western Australia approved all animal procedures. Five 19-week old transgenic mice expressing skeletal muscle α-actin with the D286G variant (herein referred to as "D286G"; (Ravenscroft et al., 2013)) and five age- and gender-matched wild-type mice (referred to as "WT") were used in the present study. Mice were killed by cervical dislocation and tibialis anterior (TA) muscles were dissected.

2.2. Muscle preparation and myofiber permeabilization

TA muscles were placed in relaxing solution at 4 °C. Bundles of approximately 50 myofibers were dissected free and then tied with surgical silk to glass capillary tubes at slightly stretched lengths. They were then treated with skinning solution (relaxing solution containing glycerol; 50:50 v/v) for 24 h at 4 °C, after which they were transferred to −20 °C. In addition, the muscle bundles were treated with sucrose, a cryoprotectant, within 1–2 weeks for long-term storage (Frontera and Larsson, 1997). They were detached from the capillary tubes and snap frozen in liquid nitrogen-chilled propane and stored at −80 °C.

2.3. X-ray diffraction recordings and analyzes

Two to three days prior to X-ray recordings, bundles were de-sucrosed and transferred to a relaxing solution, and single myofibers were dissected. Arrays of approximately 30 fibers were prepared (Iwamoto, 2009; Iwamoto et al., 2001, 2002, 2003; Ochala et al., 2012, 2008, 2011). For each myofiber, both ends were clamped to half-split gold meshes for electron microscopy (width, 3 mm), which had been glued to precision-machined ceramic chips (width, 3 mm) designed to fit into a specimen chamber. The arrays were then transferred to the skinning solution and stored at −20 °C. On the day of the X-ray recordings, arrays were placed in a plastic dish containing a pre-activating solution and washed thoroughly to remove the glycerol. Arrays were then transferred to the specimen chamber, capable of manual length adjustment and force measurement (force transducer, AE801, Memscap, Bernin, France), filled with a pre-activating solution. Mean sarcomere length was measured and set to 2.5–2.6 μm or >3.6 μm. Subsequently, for arrays at a sarcomere length equal to 2.5–2.6 μm, X-ray diffraction patterns were recorded at 15 °C, first in the pre-activating solution and then in the activating solution (pCa 4.5) when maximal steady-state isometric force was reached. It should be mentioned that the activating solution was supplied to the chamber by using a remote-controlled pump. For arrays at a sarcomere length > 3.60 μm, the protocol was identical except that pre-activating and activating solutions were replaced by low-EGTA rigor and calcium-rigor solutions with 2,3-butanedione monoxime (to prevent major sarcomere in-homogeneities). For each array, approximately 20–30 diffraction patterns were recorded (depending on fiber length) for each solution at the BL45XU beamline of SPring-8. The wavelength was 0.09 nm, and the specimen-to-detector distance was 2 m. As a detector, a cooled CCD camera (C4880, Hamamatsu Photonics; 1000 × 1018 pixels) was used in combination with an image intensifier (VP5445, Hamamatsu Photonics). To minimize radiation damage, the exposure time was kept low (2 s), and the specimen chamber was moved 100 μm after each exposure. Moreover, we placed an aluminum plate (thickness, 0.35–0.5 mm) upstream of the specimen chamber. The beam flux was estimated to be between 2.7×10^{11} and 4.0×10^{11} photons/s after attenuation, and the beam size at the sample position was 0.2 mm (vertical) and 0.3 mm (horizontal). Following the X-ray recordings, background scattering was subtracted, and reflection intensities were determined as described elsewhere (Iwamoto, 2009; Iwamoto et al., 2001, 2002, 2003; Yagi, 2003).

2.4. Solutions

Relaxing and activating solutions contained 4 mM Mg-ATP, 1 mM free Mg^{2+}, 20 mM imidazole, 7 mM EGTA, 14.5 mM creatine phosphate, 324 U/mL creatine phosphokinase, 1000 U/mL catalase, and KCl to adjust the ionic strength to 180 mM and pH to 7.0. Dithiothreitol (DTT) was also added. The pre-activating solution was identical to the relaxing solution, except that the EGTA concentration was reduced to 0.5 mM. The concentrations of free Ca^{2+} were $10^{-9.0}$ M (relaxing and pre-activating solutions) and $10^{-4.5}$ M (activating solutions). The rigor solution had similar compositions as the activating solution, except that MgATP, creatine phosphate, and creatine phosphokinase were absent.

3. Results and discussion

All the intensity changes during activation were successfully monitored and analyzed. The diffraction patterns are shown in Figs. 1 and 2. All intensities are summarized in Tables 1 and 2.

3.1. Preserved myofilament lattice

To prove that the myofilament lattice spacing was not affected by the presence of D286G skeletal muscle α-actin, we converted the 1,0 equatorial reflections to $d_{1,0}$ spacings using Bragg's Law (Colson et al., 2007). $d_{1,0}$ spacing and the widths of the 1,0 equatorial reflections ($\Delta_{1,0}$) did not appear different between WT and D286G myofibers (Table 1).

3.2. Aberrant actin structural changes

The sixth (1/5.9 nm^{-1}) and seventh (1/5.1 nm^{-1}) ALLs reflect the pitch of the left- and right-handed helices drawn through the actin monomers (Iwamoto, 2009). Upon addition of Ca^{2+}, their intensities are usually greater. This is likely to arise from individual skeletal muscle α-actin molecules modifying their shape and their helical symmetry (Bordas et al., 1999; Wakabayashi et al., 1994) via an axial compression and a closing-up between subdomains 1 and 2 and between subdomains 3 and 4 (Iwamoto, 2009). In the present study, the intensification of the sixth ALL was less pronounced in D286G when compared with WT myofibers (−58%, Fig. 1 and Table 2). This suggests that the activation-induced structural change of skeletal muscle α-actin molecules is disrupted in the presence of the "poison" D286G. The mechanisms remain

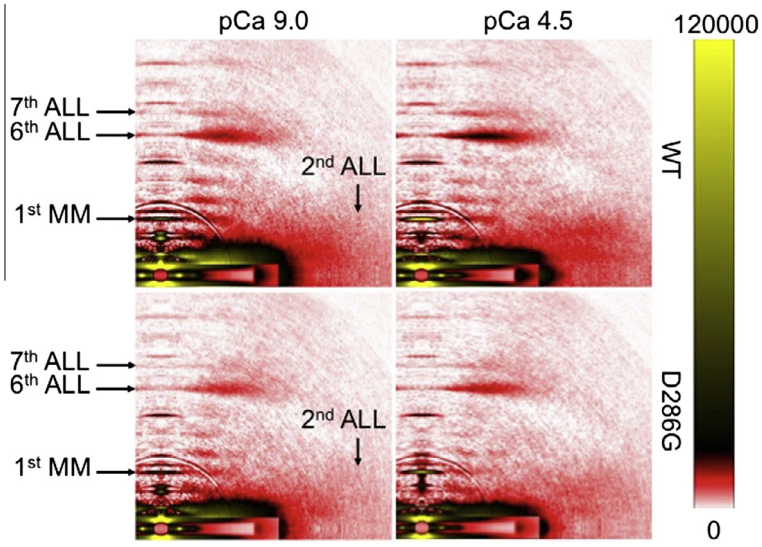

Fig. 1. X-ray diffraction patterns of myofibers from a WT mouse and from a D286G transgenic mouse. Myofibers were set at an optimal sarcomere length (2.5–2.6 μm), in pre-activating (first column, pCa 9.0) and activating (second column, pCa 4.5) solutions. MM = myosin meridional reflection; ALL = actin layer line. The color scale is linear (this applies to all patterns).

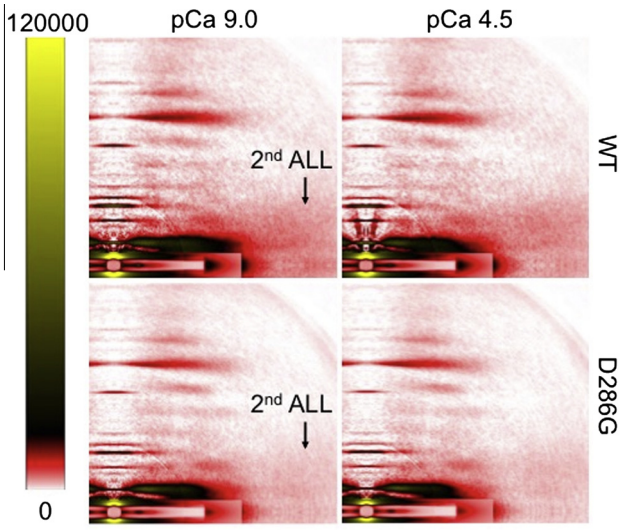

Fig. 2. X-ray diffraction of overstretched myofibers (sarcomere length > 3.6 μm) from a WT mouse and a D286G transgenic mouse. Myofibers were in low-EGTA rigor (first column, pCa 9.0) and calcium-rigor (second column, pCa 4.5) solutions. MM = myosin meridional reflection; ALL = actin layer line. The color scale is linear.

Table 1
Integrated intensities of the equatorial reflections 1,0 and 1,1. Myofibers were set at a full thin-thick filament overlap (sarcomere length of 2.5–2.6 μm).

	WT		D286G	
	pCa 9.0	pCa 4.5	pCa 9.0	pCa 4.5
$I_{1,1}$ to $I_{1,0}$ ratio	0.570	1.000	0.620	0.950
$d_{1,0}$ spacing (nm)	43.094	40.841	44.218	40.862
Peak width ($\times 10^{-4}$ nm^{-1})	7.072	9.206	7.154	9.362

unclear, but the loss of a negative charge at position 286, in subdomain 3, may locally destabilize the protein as seen for three other close-by mutations associated with cardiomyopathies, i.e., Y166C, R312H and A331P (Mundia et al., 2012). This, in turn, may promote intrinsic deficiencies by impeding the interface between actin subdomains 3 and 4 (Iwamoto, 2009). In addition, D286G may negatively affect the adjoining actin molecules. Indeed, this particular mutation is located in a loop that is known to interact with another loop positioned in subdomain 4 of the neighbouring molecule, particularly residues P241-D242-G243 (Dominguez and Holmes, 2011).

3.3. Disrupted binding of myosin molecules

The first (1/14.3 nm^{-1}) MM originates from the 14.3 nm translation between crowns of myosin heads. Its reflection depends on the average orientation of the myosin heads relative to the thick-filament backbone (Huxley et al., 1983; Reconditi et al., 2005). When myosin heads have a wide range of axial angles and are disordered, the intensity is weak. On the other hand, when strongly bound cross-bridges are formed and myosin heads ordered, the intensity increases (Huxley et al., 1983; Reconditi et al., 2005). Here, upon activation, the first MM reflection was less intense in D286G when compared with WT myofibers (−27%, Fig. 1 and Table 2). This specific D286G mutation is not directly located in a region where myosin head residues bind (Ochala et al., 2012, 2008, 2011). Hence, the observed reduction in the intensification of the first MM reflection together with the reduced $I_{1,1}$ to $I_{1,0}$ ratio (−23%, Table 1) – suggesting a limited proper strong myosin

Table 2
Integrated intensities of the major reflections presented in the recordings shown in Figs. 1 and 2. Values from activated myofibers set at a full thin-thick filament overlap (sarcomere length of 2.5–2.6 μm) are normalized using the sixth ALL data from the same relaxed myofibers. Similarly, data from overstretched activated myofibers (sarcomere length > 3.6 μm) are normalized using the sixth ALL data from the same overstretched myofibers in the absence of Ca^{2+}.

	WT		D286G	
	pCa 9.0	pCa 4.5	pCa 9.0	pCa 4.5
2nd ALL (SL 2.5–2.6 μm)	−0.023	0.135	0.001	0.103
2nd ALL (SL > 3.6 μm)	0.035	0.063	0.027	0.068
6th ALL (SL 2.5–2.6 μm)	1.000	1.208	1.000	1.086
7th ALL (SL 2.5–2.6 μm)	0.441	0.463	0.500	0.520
1st MM (SL 2.5–2.6 μm)	0.220	0.489	0.185	0.381

SL = sarcomere length; MM = myosin meridional reflection; ALL = actin layer line. Note that we found a negative value for the 2nd ALL (SL 2.5–2.6 μm – WT – pCa 9.0). This is due to the fact that the 2nd ALL reflection in relaxing solution was weak and broad and we had to subtract a noisy background.

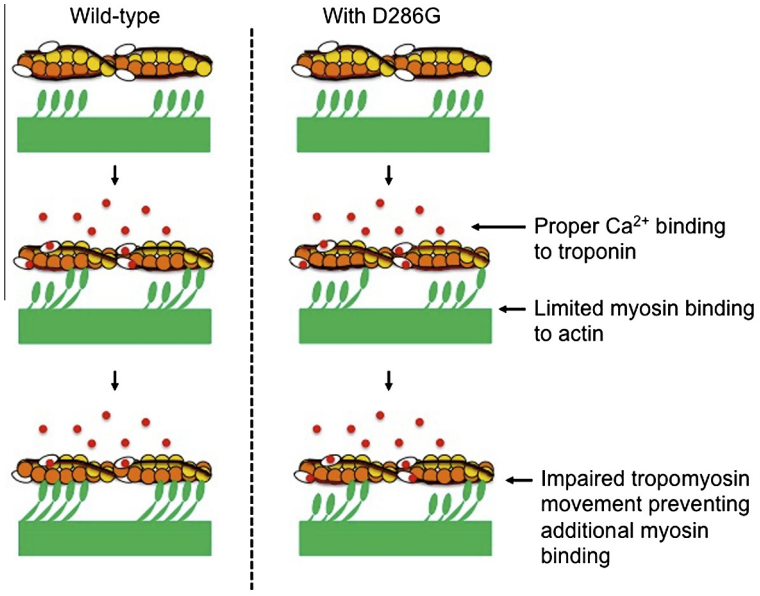

Fig. 3. Schematic view of the negative events triggered by D286G.

binding to actin molecules – are likely to arise from actin inability to undergo normal conformational modifications upon addition of Ca^{2+} (sixth and seventh ALLs, Fig. 1 and Table 2).

3.4. Altered myosin-related tropomyosin movement

To investigate whether other phenomena contribute to the contractile dysfunction, we evaluated the intensity of the far off-meridional part of the second (1/19 nm^{-1}) ALL which originates from the position of tropomyosin on the actin helix (Parry and Squire, 1973). The weaker intensity change of the second ALL in D286G when compared with WT myofibers demonstrates that tropomyosin movement over the surface of actin is partially hindered (−35%, Fig. 1 and Table 2). According to the steric model of thin filament regulation (Lehman and Craig, 2008), muscle contraction involves various tropomyosin states initiated by Ca^{2+} and then regulated by myosin molecules. When Ca^{2+} binds to the troponin complex, tropomyosin moves towards the inner domain of the thin filament, exposing sites on actin that allow weak binding of myosin cross-bridges. The weak-to-strong myosin transition induces an additional tropomyosin displacement, exposing more sites on the thin filament. This in turn permits additional binding of myosin cross-bridges, and, ultimately, leads to force production.

To evaluate whether the impaired second ALL reflection is Ca^{2+} or myosin-linked, we performed experiments where the thin-thick filament overlap was minimalized (sarcomere length > 3.6 μm) (Iwamoto, 2009). Upon addition of Ca^{2+}, the second ALL intensity change did not appear different between WT and D286G (Fig. 2 and Table 2). Thus, D286G skeletal muscle α-actin may not directly inhibit Ca^{2+}-induced tropomyosin movement, but rather indirectly down-regulate the myosin-related tropomyosin displacement by hampering the formation of strongly bound myosin cross-bridges. This is not completely unexpected as the mutation is positioned in an area which is far from residues involved in the actin-tropomyosin interaction (Li et al., 2011).

4. Conclusion

By recording and analyzing the small-angle X-ray diffraction patterns of single membrane-permeabilized myofibers from WT and D286G mice, we have been able to unravel the molecular mechanisms by which one amino acid change in the skeletal muscle α-actin protein sequence induces contractile dysfunction and weakness. In fact, we showed that upon activation, the intensity changes of the second and sixth ALLs and of the first MM reflection were only altered when the sarcomere length or thin-thick filament overlap was optimal. Consequently, the "poison" D286G does not undergo proper conformational changes upon addition of Ca^{2+}. This partially blocks the strong binding of myosin molecules impairing tropomyosin movement. Less myosin binding sites are then exposed on actin and fewer cross-bridges in the strong binding state can be further formed, overall resulting in a force deficit (Fig. 3). Interventions that would primarily restore the actomyosin interface may represent potential therapeutic strategies for the future.

Conflicts of interest

The authors have no conflicts of interest to disclose.

Acknowledgments

This study was supported by the Medical Research Council UK (to J.O.), A Foundation Building Strength for Nemaline Myopathy (G.R., K.J.N.), the Australian National Health and Medical Research Council (NHMRC; Project Grant APP1026933 to K.J.N. and G.R.) and The University of Western Australia (K.J.N., G.R., J.O.). Fellowship funding was received from the Australian National Health and Medical Research Council for G.R. (APP1035955), and the Australian Research Council for K.J.N. (FT100100734). The X-ray experiments were performed under approval of the SPring-8 Proposal Review Committee (2014A1052 and 2014B1073).

References

Bordas, J., Svensson, A., Rothery, M., Lowy, J., Diakun, G.P., Boesecke, P., 1999. Extensibility and symmetry of actin filaments in contracting muscles. Biophys. J. 77, 3197–3207.

Colson, B.A., Bekyarova, T., Fitzsimons, D.P., Irving, T.C., Moss, R.L., 2007. Radial displacement of myosin cross-bridges in mouse myocardium due to ablation of myosin binding protein-C. J. Mol. Biol. 367, 36–41.

Dominguez, R., Holmes, K.C., 2011. Actin structure and function. Annu. Rev. Biophys. 40, 169–186.

Frontera, W.R., Larsson, L., 1997. Contractile studies of single human skeletal muscle fibers: a comparison of different muscles, permeabilization procedures, and storage techniques. Muscle Nerve 20, 948–952.

Huxley, H.E., Simmons, R.M., Faruqi, A.R., Kress, M., Bordas, J., Koch, M.H., 1983. Changes in the X-ray reflections from contracting muscle during rapid mechanical transients and their structural implications. J. Mol. Biol. 169, 469–506.

Iwamoto, H., 2009. Evidence for unique structural change of thin filaments upon calcium activation of insect flight muscle. J. Mol. Biol. 390, 99–111.

Iwamoto, H., Oiwa, K., Suzuki, T., Fujisawa, T., 2001. X-ray diffraction evidence for the lack of stereospecific protein interactions in highly activated actomyosin complex. J. Mol. Biol. 305, 863–874.

Iwamoto, H., Oiwa, K., Suzuki, T., Fujisawa, T., 2002. States of thin filament regulatory proteins as revealed by combined cross-linking/X-ray diffraction techniques. J. Mol. Biol. 317, 707–720.

Iwamoto, H., Wakayama, J., Fujisawa, T., Yagi, N., 2003. Static and dynamic X-ray diffraction recordings from living mammalian and amphibian skeletal muscles. Biophys. J. 85, 2492–2506.

Lehman, W., Craig, R., 2008. Tropomyosin and the steric mechanism of muscle regulation. Adv. Exp. Med. Biol. 644, 95–109.

Li, X.E., Tobacman, L.S., Mun, J.Y., Craig, R., Fischer, S., Lehman, W., 2011. Tropomyosin position on F-actin revealed by EM reconstruction and computational chemistry. Biophys. J. 100, 1005–1013.

Mundia, M.M., Demers, R.W., Chow, M.L., Perieteanu, A.A., Dawson, J.F., 2012. Subdomain location of mutations in cardiac actin correlate with type of functional change. PLoS ONE 7, e36821.

Nguyen, M.A., Joya, J.E., Kee, A.J., Domazetovska, A., Yang, N., Hook, J.W., Lemckert, F. A., Kettle, E., Valova, V.A., Robinson, P.J., North, K.N., Gunning, P.W., Mitchell, C. A., Hardeman, E.C., 2011. Hypertrophy and dietary tyrosine ameliorate the phenotypes of a mouse model of severe nemaline myopathy. Brain.

Nowak, K.J., Ravenscroft, G., Laing, N.G., 2013. Skeletal muscle alpha-actin diseases (actinopathies): pathology and mechanisms. Acta Neuropathol. 125, 19–32.

Nowak, K.J., Wattanasirichaigoon, D., Goebel, H.H., Wilce, M., Pelin, K., Donner, K., Jacob, R.L., Hubner, C., Oexle, K., Anderson, J.R., Verity, C.M., North, K.N., Iannaccone, S.T., Muller, C.R., Nurnberg, P., Muntoni, F., Sewry, C., Hughes, I., Sutphen, R., Lacson, A.G., Swoboda, K.J., Vigneron, J., Wallgren-Pettersson, C., Beggs, A.H., Laing, N.G., 1999. Mutations in the skeletal muscle alpha-actin gene in patients with actin myopathy and nemaline myopathy. Nat. Genet. 23, 208–212.

Ochala, J., Ravenscroft, G., Laing, N.G., Nowak, K.J., 2012. Nemaline myopathy-related skeletal muscle alpha-actin (ACTA1) mutation, Asp286Gly, prevents proper strong myosin binding and triggers muscle weakness. PloS one 7, e45923.

Ochala, J., Iwamoto, H., Larsson, L., Yagi, N., 2008. A myopathy-linked tropomyosin mutation severely alters thin filament conformational changes during activation. Proc. Natl. Acad. Sci. USA 107, 9807–9812.

Ochala, J., Lehtokari, V.L., Iwamoto, H., Li, M., Feng, H.Z., Jin, J.P., Yagi, N., Wallgren-Pettersson, C., Penisson-Besnier, I., Larsson, L., 2011. Disrupted myosin cross-bridge cycling kinetics triggers muscle weakness in nebulin-related myopathy. FASEB J.

Parry, D.A., Squire, J.M., 1973. Structural role of tropomyosin in muscle regulation: analysis of the X-ray diffraction patterns from relaxed and contracting muscles. J. Mol. Biol. 75, 33–55.

Ravenscroft, G., McNamara, E., Griffiths, L.M., Papadimitriou, J.M., Hardeman, E.C., Bakker, A.J., Davies, K.E., Laing, N.G., Nowak, K.J., 2013. Cardiac alpha-actin over-expression therapy in dominant ACTA1 disease. Hum. Mol. Genet. 22, 3987–3997.

Ravenscroft, G., Jackaman, C., Bringans, S., Papadimitriou, J.M., Griffiths, L.M., McNamara, E., Bakker, A.J., Davies, K.E., Laing, N.G., Nowak, K.J., 2011. Mouse models of dominant ACTA1 disease recapitulate human disease and provide insight into therapies. Brain 134, 1101–1115.

Reconditi, M., Linari, M., Lucii, L., Stewart, A., Sun, Y.B., Narayanan, T., Irving, T., Piazzesi, G., Irving, M., Lombardi, V., 2005. Structure-function relation of the myosin motor in striated muscle. Ann. N. Y. Acad. Sci. 1047, 232–247.

Wakabayashi, K., Sugimoto, Y., Tanaka, H., Ueno, Y., Takezawa, Y., Amemiya, Y., 1994. X-ray diffraction evidence for the extensibility of actin and myosin filaments during muscle contraction. Biophys. J. 67, 2422–2435.

Yagi, N., 2003. An X-ray diffraction study on early structural changes in skeletal muscle contraction. Biophys. J. 84, 1093–1102.